

# Phantom: Untargeted Poisoning Attacks on Semi-Supervised Learning (Full Version)\*

Jonathan Knauer  
jonathan.knauer@stud.tu-darmstadt.de  
Technical University of Darmstadt  
Germany

Hossein Fereidooni  
hossein.fereidooni@kobil.com  
KOBIL GmbH  
Germany

Phillip Rieger  
phillip.rieger@trust.tu-darmstadt.de  
Technical University of Darmstadt  
Germany

Ahmad-Reza Sadeghi  
ahmad.sadeghi@trust.tu-darmstadt.de  
Technical University of Darmstadt  
Germany

## ABSTRACT

Deep Neural Networks (DNNs) can handle increasingly complex tasks, albeit they require rapidly expanding training datasets. Collecting data from platforms with user-generated content, such as social networks, has significantly eased the acquisition of large datasets for training DNNs. Despite these advancements, the manual labeling process remains a substantial challenge in terms of both time and cost. In response, Semi-Supervised Learning (SSL) approaches have emerged, where only a small fraction of the dataset needs to be labeled, leaving the majority unlabeled. However, leveraging data from untrusted sources like social networks also creates new security risks, as potential attackers can easily inject manipulated samples. Previous research on the security of SSL primarily focused on injecting backdoors into trained models, while less attention was given to the more challenging untargeted poisoning attacks. In this paper, we introduce *Phantom*, the first untargeted poisoning attack in SSL that disrupts the training process by injecting a small number of manipulated images into the unlabeled dataset. Unlike existing attacks, our approach only requires adding few manipulated samples, such as posting images on social networks, without the need to control the victim. *Phantom* causes SSL algorithms to overlook the actual images' pixels and to rely only on maliciously crafted patterns that *Phantom* superimposed on the real images. We show *Phantom*'s effectiveness for six different datasets and 3 real-world social-media platforms (Facebook, Instagram, Pinterest). Already small fractions of manipulated samples (e.g., 5%) reduce the accuracy of the resulting model by 10%, with higher percentages leading to a performance comparable to a naive classifier. Our findings demonstrate the threat of poisoning user-generated content platforms, rendering them unsuitable for SSL in specific tasks.

## KEYWORDS

Deep Neural Network, Semi-Supervised-Learning, Poisoning

## ACM Reference Format:

Jonathan Knauer, Phillip Rieger, Hossein Fereidooni, and Ahmad-Reza Sadeghi. 2024. Phantom: Untargeted Poisoning Attacks on Semi-Supervised Learning (Full Version)\*. In *Proceedings of the 2024 ACM SIGSAC Conference on Computer and Communications Security (CCS '24)*, October 14–18, 2024, Salt Lake City, UT, USA. ACM, New York, NY, USA, 17 pages. <https://doi.org/10.1145/3658644.3690369>

## 1 INTRODUCTION

Deep Neural Networks (DNNs) have been rapidly evolving with spectacular abilities, such as DALL-E [46], DeepFakes [39], and the chatbot ChatGPT [40], to name a few. Simultaneously, DNNs are increasingly used also for safety-critical domains, such as self-driving cars, necessitating exceptionally high reliability and precision. However, with the growing complexity of these tasks, also the size of the DNNs and the number of trainable parameters grow significantly. To effectively train these DNN models, the required amount of training data is growing rapidly. One possible source of large amounts of training data is the Internet, where large amounts of user-generated content are available on platforms such as Instagram (image data), Reddit (text data), and YouTube (video data). Thus, the data that were uploaded on these platforms became a high-value asset, as different actors, such as companies, can use these data to train DNNs.

However, labeling the data remains a significant practical challenge in terms of cost and time. To address this issue, recent research has focused on developing algorithms that either avoid the need for labeling entirely or minimize the number of samples that require manual annotation.

Notably, recent news about the achievements of DNNs focus on Large Language Models (LLMs) that are trained in early training phases on text sequences in a self-supervised manner. However, these models still require labeled training data for later supervised training phases [41, 42, 45]. Furthermore, other applications, such as image recognition or those developed by stakeholders such as small companies or academic institutions [18], typically do not rely exclusively on self-supervised training methods. This shows the ongoing need for labeled training data, despite significant progress in self-supervised learning approaches.

Publication rights licensed to ACM. ACM acknowledges that this contribution was authored or co-authored by an employee, contractor or affiliate of a national government. As such, the Government retains a nonexclusive, royalty-free right to publish or reproduce this article, or to allow others to do so, for Government purposes only.

CCS '24, October 14–18, 2024, Salt Lake City, UT, USA

© 2024 Copyright held by the owner/author(s). Publication rights licensed to ACM.  
ACM ISBN 979-8-4007-0636-3/24/10...\$15.00  
<https://doi.org/10.1145/3658644.3690369>

\* © Knauer 2024. This is the author's version of the work. It is posted here for your personal use. Not for redistribution. The definitive version was published in CCS2024, <https://doi.org/10.1145/3658644.3690369>.

### Semi-Supervised Learning.

Semi-Supervised Learning (SSL) algorithms avoid the problem of time-intensive labeling the obtained large dataset by minimizing the number of labeled samples that are required for the training algorithm. SSL algorithms utilize two datasets, a small labeled dataset and a large unlabeled dataset. The model is initially trained only on the labeled dataset, while the current model is simultaneously used to predict the labels for samples from the unlabeled dataset. Once the model predicts the labels for some samples with high confidence, these samples are used with these guessed labels for further training. Current state-of-the-art algorithms for SSL include MixMatch [5], UDA [62], and FixMatch [55]. These algorithms are highly effective at leveraging only a small number of labeled samples to achieve a performance comparable to fully supervised methods. For example, on the CIFAR-10 benchmark dataset, labeling a only 40 out of 50 000 samples is sufficient to achieve decent accuracy levels. SSL algorithms allow leveraging large unlabeled datasets, e.g., downloaded from social media platforms, while avoiding the costly and time-consuming process of manual labeling.

**Attacks on SSL.** However, despite the benefits of leveraging large datasets from platforms with user-generated content, using untrusted data also creates new attack vectors. If a party like a company utilizes the user-generated data of such a platform, an attacker can easily upload maliciously crafted images to the platform to manipulate DNNs that are trained on this data. Recent research proposed attacks that insert manipulated samples into the unlabeled training data to inject a backdoor into the trained model. The backdoor causes the trained DNN to misbehave in a well-defined manner, such as classifying selected images as belonging to a different class chosen by the attacker [7, 12]. Previous work developed untargeted poisoning attacks that reduce the trained model's accuracy by manipulating the labeled dataset [19, 32]. However, to manipulate the labeled samples, a strong control over the attacked victim is required. Thus, this would also enable the adversary to interfere directly with the training process.

While existing untargeted poisoning attacks assume access to the labeled dataset, to the best of our knowledge, no untargeted attack has been proposed that manipulates the unlabeled data to disrupt the training process. Compared to backdoor attacks that manipulate the unlabeled dataset [7, 12], untargeted poisoning attacks pose significant challenges. In backdoor attacks, the DNN model can achieve both objectives simultaneously, a decent performance on the benign data and injecting the backdoor. Backdoor attacks only add an additional, undesired function to the DNN. Consequently, the poisoned data only need to provide examples for this additional function such that if the DNN is trained on these data, it will also learn this function. In contrast, untargeted poisoning attacks, which aim to compromise the performance on benign test data, present a more challenging scenario as here both above-mentioned objectives will be in direct conflict with each other. Thus, one of the challenging aspects when designing untargeted attacks is the necessity for a relatively small number of samples to overrule the impact of a large number of benign samples.

Another challenge is the lack of information about the SSL algorithm, DNN architecture, or used model weights. As the manipulated samples must be crafted and uploaded to the platform with user-generated content before the actual training starts, the attack

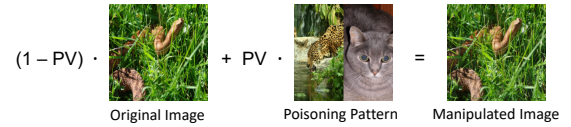


**Figure 1: Example for poisoned image construction as a combination of the unpoisoned image and the Poisoning Pattern, weighted by the Pattern Visibility (PV) parameter, here 0.1.**

has to be executed blindly. Moreover, generating inaccurate labels for the manipulated data remains another challenge since the labels for the unlabeled dataset are obtained by the SSL algorithm during the training.

**Our goal and contributions.** In this paper, we propose *Phantom*, the first blind untargeted poisoning attack on SSL that disrupts the training by manipulating the unlabeled dataset. By adding a small number of manipulated samples to the unlabeled dataset, such as uploading manipulated images to a social network, *Phantom* significantly reduces the performance of the trained model. To effectively disturb the SSL algorithm, we incorporate a hidden pattern (a *Phantom*) into the manipulated samples, causing the algorithms to overlook the actual content (e.g., original pixels) and rely only on hidden patterns that we superimposed on the original content for guessing the unlabeled samples' labels. This causes the SSL algorithm to mislabel the manipulated samples and, in turn, negatively impacts the training and prevents the utilization of benign samples. An example, using images as a demonstration, is illustrated in Fig. 1. Here, the DNN uses a part of the poisoning pattern, such as the tiger or cat, to predict the label while primarily using the snake for loss calculation and parameter adaption.

It is worth noting that even with a small percentage of manipulated data, such as 5%, the accuracy of the resulting model can be reduced by 10%. We demonstrate that untargeted poisoning attacks can be made without making any assumptions, such as strong control or the ability to monitor the victim. Thereby, we show that untargeted poisoning attacks pose a practical and realistic threat.

In summary, our contributions include:

- We propose *Phantom*, the first untargeted poisoning attack that disrupts the training of SSL algorithms and reduces the model's utility by only adding few samples to the unlabeled dataset without requiring any knowledge of the SSL algorithm, DNN structure, or hyperparameters. In contrast to backdoor attacks, where the benign and backdoor objectives can be achieved in parallel, *Phantom* overrules the benign majority of samples to reduce the model's utility. *Phantom* poisons sources for unlabeled data, making them unusable for SSL training in certain tasks (Sect. 4.2).
- We design a scheme for manipulating samples that takes advantage of the model's overfitting on the labeled dataset in the initial stages of training. This causes the SSL algorithms to ignore the original sample and entirely rely on superimposed patterns, thus mislabeling the sample (Sect. 4).
- We conduct an extensive evaluation and demonstrate that already 5% of manipulated data can lead to a significant reduction in the performance of the trained model by 10%. We effectively show the efficacy of *Phantom* across a range of state-of-the-art SSL algorithms, datasets, and parameter configurations and its

resistance to data augmentation techniques and countermeasures against adversarial examples. Additionally, we thoroughly examine the attack's impact on the model's behavior in-depth using explainable AI techniques (Sect. 5).

- To demonstrate the risks posed by the *Phantom* attack and the need for robust SSL algorithms, we show its effectiveness through a real-world case study. We utilize data extracted from three major social networks — Facebook, Instagram, and Pinterest — which host user-generated content and are plausible sources for SSL training data (Sect. 5.6).

## 2 BACKGROUND

In the following sections, we provide an overview of the necessary background for the rest of the paper. In Sect. 2.1, we introduce several state-of-the-art SSL algorithms (MixMatch [5], UDA [62], and FixMatch [55]), which will be used in this paper. These algorithms are chosen for their popularity and effectiveness in various SSL tasks. Later, we describe and categorize different attacks that target DNN models during the training phase (Sect. 2.2). Further, in App. A, we describe an overview of data augmentation techniques that are commonly employed in the field of SSL.

### 2.1 Semi-Supervised Learning

Semi-Supervised Learning (SSL) is a class of algorithms that utilize a combination of a small labeled dataset, denoted as  $\mathcal{X}$ , and a much larger unlabeled dataset, denoted as  $\mathcal{U}$ , where  $|\mathcal{X}| \ll |\mathcal{U}|$ , to train a Machine Learning model for classification tasks, such as a Deep Neural Network (DNN). In contrast, non-SSL algorithms require the entire dataset to be labeled, which can be costly in terms of time and expertise. SSL algorithms only require a small portion of the dataset to be labeled. The labeled part  $\mathcal{X}$  is used for the initial training of the DNN and to make educated guesses about the labels of the unlabeled data during training. In this work, we exemplarily focus on the algorithms MixMatch [5], UDA [62], and FixMatch [55], as these have been shown to achieve the best performance for image applications [7].

**MixMatch** generates for each unlabeled sample  $u \in \mathcal{U}$ , i.e., an image, multiple augmented versions and averages the predictions of the current model to obtain a guess for the probability distribution for the label of  $u$ . For a sample  $u \in \mathcal{U}$  the probability distribution  $p_u$  is represented as a vector. For each possible label (or category)  $c \in \mathcal{C}$ , the respective element  $p_{u,c}$  indicates the probability that  $u$  belongs to  $c$ . This guessed probability distribution is then sharpened based on a temperature parameter  $T$  as:

$$\text{Sharpen}(p_u, T)_i = \frac{p_{u,i}^{1/T}}{\sum_{c \in \mathcal{C}} p_{u,c}^{1/T}} \quad (1)$$

The loss  $\mathcal{L} = \mathcal{L}_{\mathcal{X}} + \lambda_{\mathcal{U}} \mathcal{L}_{\mathcal{U}}$  is then defined as the sum of the binary-cross-entropy loss  $\mathcal{L}_{\mathcal{X}}$  for the labeled training data  $\mathcal{X}$ , and the distance  $\mathcal{L}_{\mathcal{U}}$  between the predictions for the augmented unlabeled samples  $u \in \mathcal{U}$  to the sharpened guessed label. The unlabeled data's loss is in addition weighted by a hyperparameter  $\lambda_{\mathcal{U}}$  [5].

#### UDA

also generates multiple augmented versions of each unlabeled sample to guess the correct label. However, UDA uses different types

of augmentations, one for guessing the label and another for calculating the loss. To guess the label, UDA applies weak augmentation to the sample, while for the loss calculation, it uses strong augmentation, causing stronger deformations of the images. The loss for the unlabeled example is based on the prediction of the strongly augmented version. The algorithm optimizes the parameters of the DNN to make the prediction of the strong augmented sample match the label that was predicted for the weakly augmented versions. Additionally, UDA only uses samples where the confidence for the prediction is higher than a configurable threshold [62].

#### FixMatch

builds on UDA by also using different augmentation types for guessing the label and for minimizing the loss. However, unlike UDA, FixMatch does not sharpen the probability distribution of the guessed label. Instead, it selects the label with the highest score and uses a one-hot encoding of this label [55].

### 2.2 Poisoning Attacks

Attacks that alter the training data of a DNN are often referred to as poisoning attacks [7, 16, 17, 19, 67]. Such attacks can be classified into the following categories:

#### Targeted Poisoning:

In this type of attack, the attacker aims to manipulate the DNN's predictions towards a specific target class for certain samples. Thus, targeted attacks inject a hidden function within the DNN. Some literature [7] subdivides this attack type into two subcategories. The first subcategory involves attacks that cause the DNN to misclassify only a fixed set of samples. Attacks in the second subcategory cause the DNN to misclassify all samples with a specific trigger, such as the presence of a certain colored patch or object in an image.

#### Untargeted Poisoning:

This category of attacks aims to degrade the overall performance of the DNN on all input samples by reducing its accuracy to that of a simple or naive model. This is different from targeted attacks, where the goal is to make the DNN misclassify only specific samples. The challenge in untargeted attacks is that their objective is to negatively impact the performance of the DNN on all data, including non-poisoned samples. In targeted attacks, the DNN can have a high accuracy on non-poisoned data and still misclassify the targeted samples. Thus, in targeted attacks both, the objective from benign data, to learn recognizing images, as well as the objective of the targeted attacks, of misclassifying the backdoor samples, can be achieved. In comparison, in untargeted attacks, either the attack is successful or the model achieves a decent performance on the benign training data. Therefore, the manipulated samples here need to counteract the benign data.

## 3 PROBLEM SETTING

In the following, we describe the considered system (Sect. 3.1), define the threat model (Sect. 3.2), and describe the challenges that untargeted attacks face in SSL (Sect. 3.3).

### 3.1 System Setting

We consider a system where anonymous clients upload user-generated content, such as images, to an internet platform, denoted as  $\mathcal{P}$ . Real-world examples of such platforms are social media websites, such

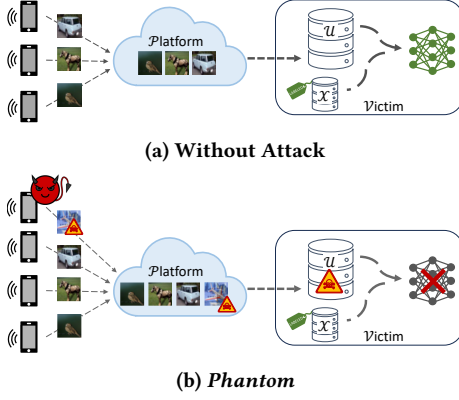


**Figure 2: Overview of the considered system where the Victim downloads data from a Platform with user-generated content to obtain an unlabeled dataset ( $\mathcal{U}$ ) that is used with a small labeled dataset ( $\mathcal{X}$ ) to train a DNN**

as Instagram, Facebook, or Pinterest. The platform  $\mathcal{P}$  may perform modifications on the content, such as compressing images to reduce their size. Afterward, the victim  $\mathcal{V}$  accesses the publicly available content on  $\mathcal{P}$  to obtain a large dataset, referred to as  $\mathcal{U}$ , for training a DNN using a SSL algorithm of their choice. In addition to  $\mathcal{U}$ ,  $\mathcal{V}$  also uses a small dataset, referred to as  $\mathcal{X}$ , that has been labeled manually. Since the process of labeling is time-consuming and requires human effort, it is assumed that  $|\mathcal{X}| \ll |\mathcal{U}|$ . Figure 2 illustrates the considered system.

### 3.2 Threat Model

We consider a weak adversary  $\mathcal{A}$ , whose only capability is the ability to upload data to a public platform  $\mathcal{P}$  hosting user-generated content.  $\mathcal{A}$  aims to prevent the victim  $\mathcal{V}$  from training a model on data that is uploaded to  $\mathcal{P}$ . The purposes of such attacks might include disrupting  $\mathcal{V}$ , for instance, if  $\mathcal{A}$  and  $\mathcal{V}$  are competing entities, or preventing parties from utilizing the data that is available on  $\mathcal{P}$ . In the latter case,  $\mathcal{A}$  could have commercial goals, e.g., revealing the poisoned samples only after  $\mathcal{V}$  pays a ransom.  $\mathcal{A}$ 's objective can be formulated as follows:

**Adversary's Objective** is to significantly<sup>1</sup> decrease the utility of DNN models that are trained in a semi-supervised manner on  $\mathcal{U}$ .

As  $\mathcal{P}$  is a public platform with user-generated content, it is sufficient for  $\mathcal{A}$  to control at least one client, such as a mobile phone or a computer. We, therefore, assume that  $\mathcal{A}$  can use such a client to upload content to  $\mathcal{P}$ . Also, we assume that  $\mathcal{A}$  can make educated guesses for some labeled samples from  $\mathcal{X}$ . It is important to note that  $\mathcal{A}$  does not need to guess the samples in  $\mathcal{X}$  with high precision. If  $\mathcal{A}$  has a set  $\mathcal{X}_{\mathcal{A}}$  of samples where it suspects that some of them are part of  $\mathcal{X}$ , it is sufficient if there is some overlap, thus

<sup>1</sup>There exists no precise threshold which performance drop can be considered to be significant as this depends on the domain. In safety-critical applications, such as self driving cars, even a drop by 1% already can make the model unusable, while in applications recognizing pictures on smartphones 1% can be tolerated. We elaborate on this in Sect. 6.1.

$\mathcal{X}_{\mathcal{A}} \cap \mathcal{X} \neq \emptyset$ . Given the widely available and well-known datasets, e.g., for image recognition and the fact that  $\mathcal{A}$  can try many samples, it is reasonable to assume that at least some of the guessed samples in  $\mathcal{X}_{\mathcal{A}}$  are correct (see Sect. 5.4).

However, we do not make any assumptions about the training process.  $\mathcal{A}$  can only augment the unlabeled dataset but lacks knowledge of the used algorithms, DNN architecture, or training specifics. Neither can  $\mathcal{A}$  affect these parameters nor can  $\mathcal{A}$  monitor the training process. Thus  $\mathcal{A}$  performs a black-box attack. Additionally,  $\mathcal{A}$  is unable to manipulate the labeled samples in  $\mathcal{X}$ , delete samples from  $\mathcal{U}$ , or modify non-poisoned samples. The only action that  $\mathcal{A}$  can take is adding samples to  $\mathcal{U}$ .

Notably, we do not assume that the adversary  $\mathcal{A}$  has any insight into the active training process of the victim  $\mathcal{V}$ . Consequently,  $\mathcal{A}$  cannot directly verify the success of the attack and must instead estimate its effectiveness through prior simulations, similar to existing work on adversarial deep learning [31, 52, 53]. This aspect will be further discussed in Sect. 6.2.

### 3.3 Challenges

In SSL, it is not practical to make strong assumptions about the adversary  $\mathcal{A}$ . Instead,  $\mathcal{A}$  has to operate blindly and perform the attack, i.e., upload the images to a platform  $\mathcal{P}$ , without knowing any details about the training (SSL algorithm, DNN architecture, training parameters, etc.). In contrast to existing work [19, 32], we consider an adversary  $\mathcal{A}$  that does not have these details. Instead,  $\mathcal{A}$  aims to negatively affect the performance of the trained model only by uploading samples to a publicly accessible platform that is designed for hosting user-generated content. This open threat scenario poses a number of significant challenges that we describe in the following:

#### C1 - Prevent utilization of non-manipulated samples:

Given the assumption that  $\mathcal{A}$  cannot manipulate the samples uploaded by benign users to  $\mathcal{P}$  but can only add additional samples to the platform, one of the main challenges is to manipulate a small number of samples in such a way that they negatively affect the ability of the training algorithm to benefit from the large number of remaining benign samples. As we show in Sect. 5.4, simply preventing the manipulated samples from contributing positively to the training is not sufficient, as there are still enough benign samples for the DNN model to learn from.

**C2 - Stealthiness:** Even for small percentages of manipulated images, e.g., 10%, users will notice if many media files on social networks show a certain pattern or artifacts that are caused by the poisoning. Additionally, if humans can detect these manipulations, it would be possible to gather a sufficient number of manipulated samples to develop an automated filtering system and thus defeat the attack. Therefore, another important challenge is to stealthily manipulate the samples to evade detection by humans while still effectively disturbing the SSL training algorithm.

**C3 - Causing SSL Algorithm to mislabel samples:** Our attack makes use of wrongly labeled samples to disturb the training. However, the adversary  $\mathcal{A}$  does not have access to the labeled dataset and the labels for the unlabeled dataset are automatically determined during the training. Therefore, another challenge is to make the SSL algorithm to craft wrong labels for the manipulated samples



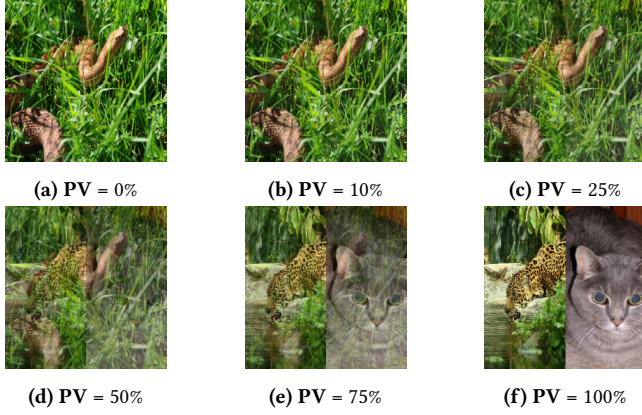


**Figure 3: Effect of different Patter Visibility (PV) rates to obtain a manipulated image for the ImageNet dataset.**

without changing the sample (i.e., images) too much, as this would affect the ability of the DNN model to learn the wrong behavior.

**C4 - Effectiveness Against Benign Majority:** Given the vast amount of content posted daily on social media, it is unrealistic to assume that  $\mathcal{A}$  can control a majority of the unlabeled samples by uploading a large number of manipulated media files. Therefore, one of the key challenges for an untargeted poisoning attack is to effectively decrease the utility of a trained model by only manipulating a small fraction of the samples. For backdoor attacks, both, the benign objective of achieving a decent performance and the attacker’s objective to inject a backdoor, can be fulfilled simultaneously. However, for untargeted poisoning attacks, the attacker’s objective of preventing the model from achieving a decent performance is in contradiction with the benign objective. Only one objective can be achieved at the same time. Therefore, a key challenge is, how to succeed against the majority of benign samples by using only a minority of samples.

## 4 PHANTOM

In the following, we introduce the *Phantom* attack. First, we describe the motivation behind the attack. Then, we first provide a high-level overview of the *Phantom* attack (Sect. 4.2 followed by a detailed explanation of the individual components (Sect. 4.3).

### 4.1 Motivation

The primary motivation for *Phantom*’s mechanism stems from the observation that SSL algorithms tend to rely heavily on the labeled data during early training epochs. Already during the early epochs of the training, the DNN achieves high accuracy on the labeled dataset  $\mathcal{X}$  (see App. C). This dependency on  $\mathcal{X}$  makes the DNN model susceptible to overfitting on the samples in the labeled dataset  $\mathcal{X}$ , which can lead to misclassification of unseen data. This phenomenon becomes particularly relevant when an input  $u \in \mathcal{U}$  contains artifacts that resemble an image from the labeled dataset  $\mathcal{X}$  with label  $l$ . In such cases, the model’s increased sensitivity to detect even parts of labeled samples causes it to predict label  $l$  for a new sample  $u$ , regardless of the actual class of  $u$ . Thus, the overfitting of the DNN results in a high sensitivity to recognizing

labeled images, even when they are present only as weak shadows within the manipulated image.

Another consequence of the DNN’s overfitting on  $\mathcal{X}$  is its tendency to predict labels with high confidence for samples that are similar to those in  $\mathcal{X}$ . As a result, these similar samples are incorporated into the training process during early epochs, while the remaining samples are only gradually added and utilized later on.

### 4.2 High-Level Overview of *Phantom*

The fundamental principle of the *Phantom* attack is to induce the SSL algorithm to generate incorrect labels for samples in the unlabeled dataset. During training, the SSL algorithm’s erroneous guesses for these labels cause the parameter optimizer to make incorrect adjustments to the DNN’s parameters, thereby reducing the model’s utility rather than improving it. To cause SSL algorithms to mislabel the unlabeled samples, *Phantom* injects a poisoning pattern into the original samples. Once the manipulated samples are crafted, they are uploaded to a platform with user-generated content, such as a social network. When the victim later crawls this platform for content and downloads media, such as images, being posted there, the manipulated samples are unknowingly incorporated into their unlabeled dataset.

The manipulated samples consist of a combination of the original sample and an individual poisoning pattern. This construction is exemplified for images in Fig. 1. The resulting image comprises two parts or layers that are placed on top of each other, the original image and the shadow, referred to as the poisoning pattern.

**Causing Wrong Label Guesses.** To influence the label guesses of the SSL algorithm with the poisoning pattern, *Phantom* exploits the tendency of SSL algorithms to overfit on samples from the labeled dataset  $\mathcal{X}$ . This overfitting makes the model highly sensitive to recognizing samples from the labeled dataset, even when they are barely visible in the image. To leverage this effect, we construct the poisoning pattern using images that resemble those in the labeled dataset. This causes the SSL algorithm to use the barely visible poisoning pattern as the basis for its label prediction, addressing challenge C3. By constructing the manipulated sample primarily from a regular sample rather than solely utilizing the poisoned pattern, the resulting sample appears also less suspicious and barely visible to human observers, as demonstrated in Fig. 1. This approach addresses C2.

**Effect on the Training Process.** Using a barely visible poisoning pattern and primarily the original image ensures that the original sample is mainly used for training. During the training process, the optimization algorithm that adapts the DNN’s weights calculates the loss and gradients based on the entire image, including its original content. Since the original sample is more prominent, it is used to train the DNN model with the wrongly guessed label. The optimizer then adjusts every parameter of the DNN to increase the probability of the guessed (wrong) label. Thus, the parameters are also changed based on the image’s primary content to maximize the probability of the current label.

As described in Sect. 4.1, samples similar to those in the labeled dataset  $\mathcal{X}$ , such as those containing parts of them, are incorporated into the training process already during the early phases. This early integration of manipulated samples affects the predicted labels for

benign data, affecting the algorithm’s ability to benefit from these data, addressing C4. The combination of the manipulated sample and the mistakenly guessed label for benign data contradicts the desired benign behavior, disrupting the training process and hindering the DNN model’s ability to effectively utilize non-manipulated data, addressing C1.

**Example.** Fig. 1 shows exemplary the process of crafting a poisoning image. The resulting image consists of an original image of a snake as well as a weak shadow of a cat and a tiger serving as the poisoning pattern. Since the superimposing of the poisoning pattern is only very weak, it is invisible to human eyes. However, the overfitting of the DNN model causes the DNN to focus on the cat and the tiger, such that this weak shadow is sufficient to classify this image as a cat (or tiger). Especially in the early phases, the DNN model is not capable of recognizing arbitrary objects, but rather it has learned to recognize specific images from the labeled dataset. As a result, the manipulated image is either labeled as a cat or as a tiger. However, once the wrong label is assigned to this image, the training process will consider the whole image. Therefore, the DNN will be trained to recognize the snake image as a cat/tiger, as the poisoning pattern is barely visible in comparison to the snake.

### 4.3 Implementation

Each manipulated sample  $m$  is created as overlay from a regular sample  $r$  and the poisoning pattern  $p$ . To construct the poisoning pattern in the image domain, *Phantom* selects for each sample  $r$  two images  $p_1, p_2$  with respective labels  $l_1, l_2$  from the set  $\mathcal{X}_A$  of images that are suspected to be part of the labeled dataset  $\mathcal{X}$ . Notably, we leverage two samples  $p_1, p_2 \in \mathcal{X}_A$  for crafting the poisoning pattern. Besides causing further distraction, this also increases the probability that one of the guesses is actually part of  $\mathcal{X}$ . We noticed during our experiments that choosing the samples  $p_1$  and  $p_2$  such that they belong to different classes ( $l_1 \neq l_2$ ) increases the attack’s effectiveness, as the ambiguous labeling causes further distraction. Additionally, targeting different classes increases the probability of triggering the model’s overfitting, leading to incorrect label predictions for the current sample.

To obtain the poisoning pattern  $p$  for image applications,  $p_1$  and  $p_2$  are first cropped at the left and right side of the image, ensuring their width is half that of  $r$ . Then, if the concatenation of these cropped images is denoted as  $p$ , the color  $c$  of the pixel on position  $x, y$  of the manipulated image  $m$  is then given by:

$$m_{x,y,c} = (1 - \text{PV}) \cdot r_{x,y,c} + \text{PV} \cdot p_{x,y,c} \quad (2)$$

The Pattern Visibility (PV) parameter controls the ratio that combines the regular sample  $r$  and the poisoned pattern  $p$ . Increasing the value makes it easier for the DNN model to spot the fractions of the labeled images, while a low PV value ensures that the manipulated images remain inconspicuous.

The impact of varying PV values on the manipulated image is shown in Fig. 3, its impact on *Phantom*’s effectiveness is evaluated in Sect. 5.3. For a PV of 100% (depicted in Fig. 3f) only the poisoning pattern is visible. As the PV value decreases from 100% to lower values, the image appears increasingly less suspicious to the human eye, making it increasingly difficult to discern the pattern (as

**Table 1: Overview of the used datasets**

Dataset	#train samples	#test samples	Model	#DNN parameters
CIFAR-10	50 000	10 000	Wide ResNet-28-2	1 469 642
MNIST	60 000	10 000	Wide ResNet-28-2	1 469 354
SVHN	604 388	26 032	Wide ResNet-28-2	1 469 642
GTSRB	26 640	12 630	Wide ResNet-28-2	1 473 899
ImageNet	1 281 167	50 000	ResNet-50	25 557 032
STL-10	105 000	8 000	Wide ResNet-37-2	5 933 770

demonstrated in Fig. 3b). However, even small PV values are capable of causing a decline in the model’s performance. For instance, a PV value of 10%, as seen in Fig. 3b, is sufficient to result in a 10% decrease in the accuracy of the trained model (see Sect. 5.2).

A challenge faced by the adversary is obtaining knowledge about the actual labeled samples. As discussed in Sect. 7, existing literature assumes unrestricted access to the labeled dataset, the ability to modify it, or even knowledge of the model’s parameters, which may not be realistic. In the case of *Phantom*,  $\mathcal{A}$  is required to guess samples  $\mathcal{X}_A$  that are present in the labeled dataset  $\mathcal{X}$ . However, only some overlap between both is necessary, i.e.,  $\mathcal{X}_A \cap \mathcal{X} \neq \emptyset$ .

In order to incorporate two labeled samples into a single sample, we employ a strategy of cropping the central portion of the labeled samples. This approach has shown to be effective as the central region of an image typically contains the most salient features. It is worth noting, however, that  $\mathcal{A}$  can manually inspect the poisoned patterns before uploading the manipulated samples. As such, if  $\mathcal{A}$  determines that the most relevant part of a labeled sample is not located in the center,  $\mathcal{A}$  can easily adapt the cropping accordingly. Also, if  $\mathcal{A}$  considers some images to be too suspicious, e.g., if the poisoned pattern can be spotted in the image, it can replace the respective poisoned image with another version, e.g., by using a different benign image as the original image.

## 5 EVALUATION

In previous sections, we introduced the *Phantom* attack, which disrupts SSL training through the addition of manipulated samples to the unlabeled dataset. In the following, we show the effectiveness of *Phantom* on six different datasets and conduct a real-world case study involving three prominent social media platforms, which are suitable data sources for SSL. In addition, we analyze in App. D changes in the behavior of the model that are caused by *Phantom* using explainable AI, specifically saliency maps for benign and poisoned input samples.

### 5.1 Experimental Setup

#### Datasets:

We employed six different datasets that are regularly utilized to evaluate DNNs, particularly research that aims to address SSL from a security perspective [7, 12, 17, 19, 63, 64]. They are summarized in Tab. 1.

*CIFAR-10* [29] includes 50 000 training images of 32×32 pixels, featuring objects and animals from 10 distinct categories. The dataset is widely utilized as a benchmark for both SSL and DNN research [7, 12, 17, 19, 63, 64].

*STL-10* is tailored explicitly for SSL and consists of 100 000 unlabeled samples, 5 000 labeled images, and 8 000 test images. All images are colored and have a resolution of 96×96 pixels [11].

*SVHN* comprises of 604 388 training images and 26 032 test images, with a resolution of 32×32 pixels [37].

*MNIST* consists of 60 000 training images showing handwritten digits, all of which are grayscale and having a resolution of 28×28 pixels [30].

*GTSRB* (German Traffic Sign Benchmark) consists of 26 640 train and 12 630 test images of different traffic signs. Each of the 43 classes represents one traffic sign, while the images themselves show them at different daytimes, perspectives, and environments (urban and countryside) [25]. The dataset was accessed via the official PyTorch integration [2].

*ImageNet* is a large, high-resolution image dataset. We use the images from the ImageNet Large Scale Visual Recognition Challenge (ILSVRC), which consists of 1,3 million training images and 50 000 test images from 1 000 different categories. The size of the images is scaled to 256×256 due to the large variety of image sizes [3].

#### Parameters:

The parameters used in this study align with the setup of Zhang *et al.* [66], where the models are trained for 256 epochs, which is sufficient for convergence. Only for ImageNet we used a larger number of epochs due to the more complex training task and larger number of trainable parameters. Since it is assumed that  $\mathcal{A}$  can only upload additional images to  $\mathcal{P}$  but cannot affect the training process, no other parameters are changed from their default values. A cosine decayed learning rate is used, initialized to 0.03, a temperature  $T$  of 0.5, and the loss weight for the unsupervised loss is set to 1.0 for FixMatch and UDA, and 100.0 for MixMatch. A confidence threshold of 0.8 is used for UDA and MixMatch. The simulation of adding poisoned images to the unlabeled dataset is done by replacing a certain fraction of the unlabeled samples with manipulated images. The ratio of manipulated unlabeled samples to the total number of unlabeled samples is referred to as the Poisoned Data Rate (PDR). To choose the number of labeled samples, we considered the number of classes and ensured that the benign setting achieved reasonable accuracy. For CIFAR-10, the labeled dataset consisted of 40 images for UDA and FixMatch. Only for MixMatch 100 labeled examples were necessary to achieve a decent performance. For STL-10 we used 100 from 105 000 for UDA and FixMatch and 250 for MixMatch. For SVHN, we utilized 40 labeled images out of 604 388 images in total, from GTSRB 129 from 26 640, for MNIST 10 out of 60 000, and for ImageNet 100 000 out of 1 281 167 images. Aligned with established work on SSL [66], we randomly selected the labeled images.

#### Experiment Environment:

We evaluate our attack on three state-of-the-art SSL algorithms: MixMatch, UDA, and FixMatch as described in Sect. 2.1. To provide a comprehensive overview of the performance of the *Phantom* attack, we evaluate the overall performance (Sect. 5.2) and perform the case study (Sect. 5.6) for all three algorithms, while the evaluation of aspects that involve a large number of experiments, such as the performance for various PDR and PV rates, consider only one algorithm respectively. For the implementation, we used the NumPy [23] and PyTorch [1] frameworks. Further, we used the

**Table 2: Basic Performance of *Phantom* for CIFAR-10.**

	MixMatch	UDA	FixMatch
Benign Scenario	74.75%	79.64%	89.10%
Only Labeled Dataset	32.23%	26.00%	26.00%
Empty Images (PDR=50%)	25.52%	70.86%	74.04%
Removing 50% samples	63.25%	50.93%	75.17%
<i>Phantom</i> (PDR=5%, PV=0.1)	64.85%	68.71%	83.68%
<i>Phantom</i> (PDR=50%, PV=0.6)	23.77%	46.85%	36.11%

**Table 3: Basic Performance of *Phantom* for STL-10.**

	MixMatch	UDA	FixMatch
Benign Scenario	63.20%	78.90%	66.83%
Only Labeled Dataset	39.53%	29.01%	29.01%
Empty Images (PDR=50%)	38.10%	72.85%	64.63%
Removing 50% samples	60.91%	68.11%	60.03%
<i>Phantom</i> (PDR=5%, PV=0.1)	60.34%	74.16%	61.63%
<i>Phantom</i> (PDR=50%, PV=0.6)	34.40%	49.16%	44.33%

SSL implementation of Zhang *et al.* [66]. The experiments were conducted on three servers, one running Debian with 1 TB memory, an AMD EPYC 7742 CPU with 64 physical cores, and 4 NVIDIA Quadro RTX 8000, another server running Ubuntu with an Intel Xeon 5318S CPU having 24 cores, 512GB main memory, and 2 Nvidia RTX A6000. Due to the high computational effort for ImageNet, we used here another server with 2 AMD EPYC 7773x CPUs, 2 TB memory, and 3 NVIDIA H100 GPUs. To ensure consistent results, all experiments for CIFAR-10, and SVHN were conducted on the first server, experiments for the STL-10, GTSRB, and MNIST datasets on the second server, and all ImageNet experiments were conducted on the third server, avoiding any minor inconsistencies due to different library versions.

## 5.2 Performance of *Phantom*

The tables 2 and 3 show the effectiveness of the *Phantom* attack on three state-of-the-art SSL algorithms (MixMatch, UDA, and FixMatch) for CIFAR-10 and STL-10. As Tab. 2 demonstrates, a PDR of only 5% is sufficient for *Phantom* to decrease the accuracy by 10% for MixMatch and UDA for CIFAR-10 and 4% on average for STL-10. With higher PDR values, the accuracy reduction becomes even more significant, with a drop to 23.77% for MixMatch, 46.85% for UDA, and 36.11% for FixMatch. The table also includes two simple baselines. For one baseline (denoted as "Empty Images" in Tab. 2) half of the images are replaced by empty (black) images. For the other baseline (denoted as "Removing 50% samples" in Tab. 2) the respective samples are removed. The results of these baselines demonstrate the superior effectiveness of the *Phantom* attack. For example, for FixMatch, using empty images or removing half of all images reduces the accuracy only to 74% and 75% respectively, while *Phantom* reduces the accuracy to 36%, which is very close to the accuracy when only the labeled dataset is used (26%). Further comparisons with baselines are provided in Sect. 5.4.

To assess the stability of the obtained results, we conducted multiple iterations of the experiments for each Semi-Supervised Learning (SSL) algorithm employing our method (*Phantom*) with varying seeds. We repeated the experiments 5 times with different seeds

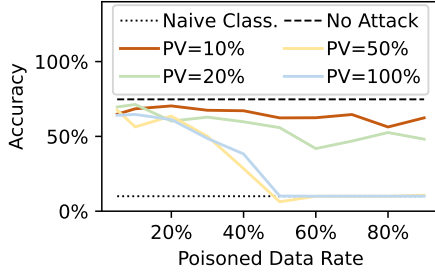


**Figure 4: Impact of the Poisoned Data Rate (PDR) for the *Phantom* attack for different Pattern Visibilities (PV) in comparison to the accuracy without attack (No Attack) and of a naive classifier (Naive Class.).**

and compared the resulting accuracies. Notably, we found that the accuracies exhibited a standard deviation of 2.6% on average across the different SSL algorithms, being negligible in comparison to the notable performance drop of almost 10% induced by *Phantom* and underscoring its robustness.

Tab. 4 shows the effectiveness of the *Phantom* attack on various datasets that are commonly used as benchmarks for SSL algorithms and attacks. As shown, *Phantom* effectively undermines the learning process for all six datasets, demonstrating its general applicability.

### 5.3 Varying Attack Parameters

The figures 4 and 5 show the effectiveness of the *Phantom* attack for different PDRs and PVs using MixMatch. As both figures illustrate, a PDR of 5% and a PV of 0.10 suffice to reduce the performance by 10% compared to the benign scenario. Both figures also show that the attack becomes more effective when using higher PDRs or higher PVs. As visible in Fig. 4, by using a PDR of 50%, the attack turns the trained model into a naive one, which always predicts the same class regardless of the input. It is worth noting that, if we use only the labeled dataset, the accuracy is still 32.23%. Therefore, without providing any incorrect labels but causing the SSL algorithm to mislabel the samples itself, the *Phantom* attack causes the resulting model to perform worse than not using any unlabeled sample.

<sup>2</sup>Due to the complex task and large number of classes, for ImageNet we use the top-5 accuracy. Thus, a sample is considered to be predicted correctly, if the true class is among the five classes with the highest predicted probabilities. Therefore, *Phantom* must not only make sure that the correct class does not receive the highest probability but that it is not even among the 5 classes with the highest predicted probabilities.

**Table 4: Effectiveness of *Phantom* for different datasets using UDA and a PDR of 5% and PV of 0.1.**

Dataset	Benign	Attack
STL-10	78.90%	74.16%
MNIST	99.20%	92.97%
SVHN	80.78%	64.87%
GTSRB	83.20%	77.78%
ImageNet <sup>2</sup>	68.08%	57.05%
CIFAR-10	79.64%	68.71%

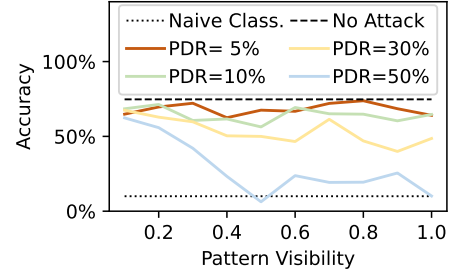


**Figure 5: Impact of the Pattern Visibility for the *Phantom* attack for different Poisoned Data Rates (PDR) in comparison to the accuracy without attack (No Attack) and of a naive classifier (Naive Class.).**

### 5.4 Ablation Study

To the best of our knowledge, *Phantom* is the first untargeted poisoning attack that does not require any control over the victim. Therefore, no similar attacks exist for comparison. To evaluate the advantage of *Phantom*, we therefore defined a number of baselines and also adapted two backdoor attacks [7, 38] to utilize them for an untargeted poisoning attack. Table 5 presents the performance of various alternative options for the *Phantom* attack, in which 10% of the data can be manipulated or removed. As shown in the table, the baseline performance of UDA, without any attack, is 79.64% accuracy. However, when utilizing only the labeled dataset, the accuracy drops to 26.00%.

For two straightforward baseline attacks, we prevent the SSL training from taking any advantage from the manipulated samples. A naive strategy would be simply not to upload these samples to the platform with user-generated content, to reduce the size of the unlabeled dataset. In this case, only the benign samples can be utilized for training. A second straightforward baseline attack to prevent the training from utilizing the manipulated images is uploading empty images, e.g., showing only black pixels. However, the results in Tab. 5 show that only preventing the model from utilizing the manipulated examples, therefore, not uploading them, is not an effective method for undermining the model. Additionally, using empty (black) images as an alternative option also demonstrates no significant impact on performance. However, it is worth noting that this strategy seems to have a regularization effect on the training process, thereby focusing the guessed probability distribution on the correct label and thus improving the model's accuracy. These experiments, therefore, showed that it is not sufficient to prevent the utilization of the manipulated samples but the utilization of the non-manipulated samples must be prevented for a successful attack (see challenge C1).

In recent years, several backdoor attacks against SSL have been developed that involve poisoning the unlabeled dataset. For a more sophisticated baseline, we adapted these approaches to make the model overfit and thus reduce the model's performance. The original backdoor attacks utilize interpolation to establish a link between samples that are intended to be mislabeled and the target samples [7, 12]. To adapt this attack and perform an untargeted poisoning attack, we inserted a colored shape on the images, causing the DNN to overfit and focus solely on the presence of this



pattern. We then utilize interpolation to create a bridge between this pattern and samples from other classes. The rationale is that the model overfits only on the pattern and unlearns other class-specific properties. Aligned with the results of Carlini [7], we use the density function  $p(x) = 1.5 - x$  for interpolation. Results using other density functions are provided in App. E.

We evaluated various baseline attacks and compared their effectiveness against *Phantom*. First, we implemented Carlini’s backdoor-ing approach [7], which interpolates between samples of different classes to misclassify samples, effectively creating a bridge between the two classes (referred to as Sample-Interpolation in Table 5). The rationale is that this interpolation might cause the SSL algorithm to incorrectly label samples, hindering its ability to accurately learn the characteristics of each class. Additionally to the attack of Carlini, we adapted several attack strategies that were originally developed for centralized learning to SSL. This included a sophisticated backdoor trigger injection technique using image warping [38] and also an adversarial-example-based attack employing the Fast Gradient Sign Method (FGSM) proposed by Goodfellow *et al.* [21]. However, as shown in Tab. 5, all three attacks were ineffective. Specifically, the FGSM attack reduced the accuracy only to 76.86% (PDR=5%) or 74.34% (PDR=10%), while *Phantom* reduced the accuracy to 68.71% (PDR=5%) and 67.15% (PDR=10%). The backdoor-inspired attacks failed, most likely due to the fact that in an untargeted poisoning attack, it is not sufficient to add a bridge to the data for making a few, well-defined samples misclassified. For the FGSM attack, the inability to prevent the utilization of the benign samples, given that the attacker controls only a small fraction of the unlabeled dataset  $\mathcal{U}$ , contributed to its failure. The attack needs to prevent the utilization of benign data to succeed (see C1), since the attack objective (preventing high accuracy) contradicts the benign objective (achieving high accuracy), which is given by the majority of the data. Simply connecting a few samples from specific classes or preventing the utilization of a few samples is, therefore, insufficient. In comparison, *Phantom* exploits the model’s overfitting on the labeled dataset  $\mathcal{X}$  and causes the model to mislabel the unlabeled samples.

Also the baseline of removing the manipulated images from the dataset has a negligible impact on performance. A reason might be that, even after removal, still enough samples remain that can be used for training the DNN. This emphasizes that it is not sufficient to prevent the poisoned samples from being used it is necessary that the manipulated samples affect the ability to utilize the other samples in the unlabeled datasets, which were not manipulated. In comparison to these baselines, *Phantom* reduces the performance by more than 12% compared to the baseline performance, demonstrating its effectiveness in not only rendering the manipulated samples unusable but also preventing the training algorithm from utilizing a significant portion of the non-manipulated images.

The table also shows the accuracy when the attacker utilizes a pattern that is composed of 4 images, with only one of them being a part of the labeled dataset. This scenario is particularly relevant in situations when the attacker must infer the labeled samples based on typical datasets for the targeted application. As the table shows, this attack is still effective and causes a significant drop in the accuracy. In addition, we performed an experiment where the set  $\mathcal{X}_{\mathcal{A}}$ , containing the samples that the adversary believes to be used

**Table 5: Effectiveness of different variations of *Phantom* for a PDR of 10%.**

Attack	UDA
Benign Scenario	79.64%
Use only Labeled Dataset	26.00%
Two-unlabeled attack	79.92%
Empty Images	89.06%
Remove 10% Samples	77.01%
Sample-Interpolation [7]	81.03%
Warp Trigger [38]	78.11%
FGSM [21]	74.34%
Three-Unlabeled-One-Labeled	71.72%
<i>Phantom</i> (PV=0.2, PDR=10%)	67.15%
<i>Phantom</i> (PV=0.1, PDR=5%)	68.71%

**Table 6: Performance of *Phantom* for CIFAR-10 if 10% of the labeled data are guessed correctly (precision=10% and sensitivity=10%) using PDR=5% and PV=0.1.**

	MixMatch	UDA	FixMatch
Benign Scenario	74.75%	79.64%	89.10%
<i>Phantom</i>	64.85%	68.71%	83.68%
<i>Phantom</i> Reduced Overlap	70.04%	73.71%	84.60%

as labeled samples, overlaps only by 20% with the set  $\mathcal{X}$  of the actual labeled samples. Here, *Phantom* still reduced the model’s utility to 71.38%.

In addition, we evaluated also scenarios, where the attacker’s guesses about the labeled dataset  $\mathcal{X}$  are made with low precision and sensitivity. Particularly, only 10% of the suspected samples  $\mathcal{X}_{\mathcal{A}}$  are actually contained in  $\mathcal{X}$  (precision=10%), while the correctly guessed samples make only 10% of the actually labeled dataset  $\mathcal{X}$  (sensitivity=10%). As Tab. 6 shows, although with reduced ability to guess the labeled samples, *Phantom* remains effective, as the accuracy is still reduced by approx. 5%.

## 5.5 Potential Countermeasures

The poisoning pattern of *Phantom* shows some similarities to adversarial examples (see Sect. 6.4). In the following, we evaluate *Phantom*’s effectiveness in the presence of potential countermeasures. Zantedeschi *et al.* proposed applying Gaussian noise on the inputs [65]. However, as shown in Tab. 10, the noise does not mitigate the attack. Pang *et al.* proposed analyzing the states of the final hidden layer for a sample  $x$  to determine if  $x$  contains an adversarial pattern [43]. Given the predicted label  $y$ , all training samples  $X_y$  having the label  $y$ ,  $f_z$  the current model until the final hidden layer, and the Gaussian Kernel  $k(\cdot, \cdot)$ , then the K-density score  $KD(x)$  for  $x$  is defined as:

$$KD(x) = \frac{1}{|X_y|} \cdot \sum_{x_i \in X_y} k(f_z(x), f_z(x_i)) \quad (3)$$

Since the thresholding test was developed for scenarios where fully labeled data are available, we used the softmax label of the training data to craft  $X_y$ . Fig. 6 shows the distribution of scores for benign and poisoned images using a PDR of 5% and different PV values after the model was trained for 10 epochs. As the figure shows,

**Table 7: Effectiveness of DNN Classifier in recognizing *Phantom* attack in terms of True Negative Rate (TNR), True Positive Rate (TPR), Precision (PRC), F1-Score, and Accuracy (ACC) for different Pattern Visibilities (PV).**

PV	TPR	PRC	F1-Score	ACC
10%	44.52%	73.62%	55.49%	64.28%
20%	68.94%	81.20%	74.57%	76.49%
50%	86.23%	84.39%	85.30%	85.14%
75%	73.82%	82.23%	77.80%	78.93%
100%	8.90%	35.81%	14.26%	46.47%

the distribution of scores for benign and manipulated samples are indistinguishable for  $PV \leq 50\%$ , and only for larger PVs could the metric identify some values. Notably, for such a high PV value, humans can already identify the manipulated images easily (see Fig. 3).

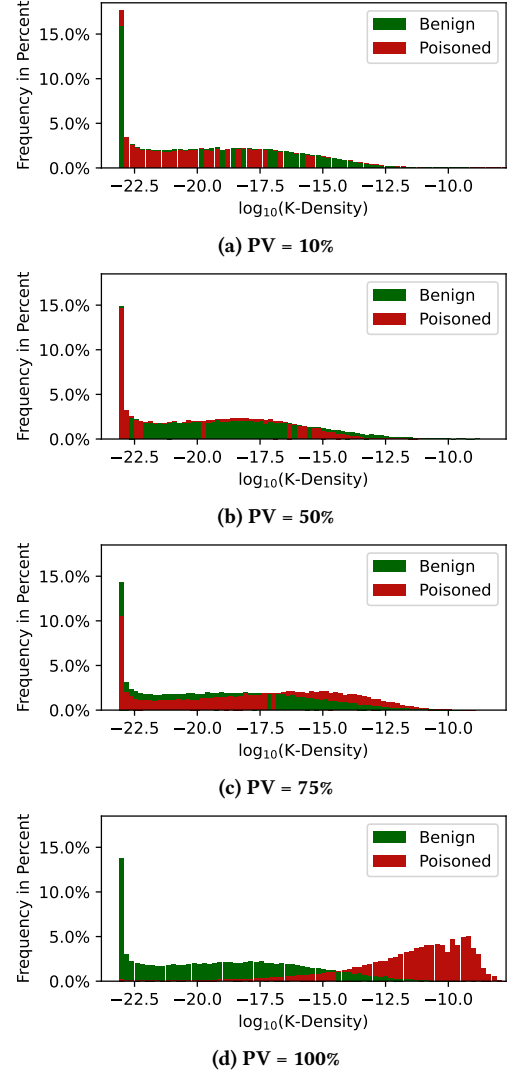
We also trained a dedicated CNN classifier using the VGG-11 architecture. We trained the classifier on benign and poisoned CIFAR-10 samples and cross-evaluated them on benign and poisoned ImageNet samples (1.2M samples each). We measured the ratio of manipulated samples that are detected (True Positive Rate, TPR), the ratio of manipulated samples compared to the total number of samples that are classified as manipulated (Precision, PRC), F1-Score, and the overall ratio of correctly classified samples (Accuracy, ACC). As Tab. 7 shows, the classifier was barely able to recognize samples for low PV values (TPR=44.52%) and only for large PV values the classifier is effective. Notably, for PVs that are too large, the effectiveness is reduced again, showing that the classifier learned to detect the sample overlay.

## 5.6 Case-Study

In addition to the aforementioned evaluation, we also conducted a case study to assess the effectiveness of our attack in a real-world scenario. Specifically, we uploaded manipulated images to three real-world social media platforms (Facebook, Instagram, and Pinterest) and evaluated how the platforms' image processing pipelines affect *Phantom*'s performance. To ensure that our experiments do not negatively impact other parties, we ensured that the images were only accessible to us by setting the privacy settings accordingly (see App. B). Due to the limited number of images that can be uploaded<sup>3</sup> to Instagram and Pinterest, we stacked multiple images to form a larger image with a higher resolution, which was then split again after uploading and downloading. Since Instagram only allowed squared images, we padded the images using black pixels and removed the padding after the download. Additionally, Instagram and Pinterest might change the image scaling if it differs from the desired sizes. Therefore, we used a size of 612×612 pixels for our images, as this size remained consistent.

As Tab. 8 shows, the *Phantom* attack is effective for the data that were obtained from all three social networks. *Phantom* reduces the accuracy of the trained model by 10%. Only in two cases, for UDA the accuracy is reduced only by 5% (Facebook) or 7% (Instagram). On the other side, for Instagram using FixMatch, the accuracy is

<sup>3</sup>Notably, as described in Sect. 6.1, an attacker could also use a script to upload each image automatically. However, as the usage of bots is clearly forbidden by these platforms, for our evaluation, we chose the batch strategy instead.

**Figure 6: Distribution of kernel density scores (K-Density) [43] for benign and poisoned images using different Pattern Visibilities (PVs).**

reduced by more than 25%. Therefore, the augmentation, such as compression, that these social networks apply does not significantly affect *Phantom*'s impact.

## 5.7 Partial Knowledge on Output Space

Recently, Richards *et al.* described the challenge of partial knowledge of the output space [47]. For crafting the poisoning pattern, it is important that the patterns' labels differ from the ground truth label of the original image. To evaluate the effectiveness of *Phantom* under limited knowledge of the output space, we tested *Phantom* in two scenarios where the individual classes of CIFAR-10 were

**Table 8: Effectiveness of *Phantom* in terms of accuracy for the CIFAR-10 dataset after downloading attack samples from different real social networks and comparison baselines.**

Scenario	FixMatch	MixMatch	UDA
Benign Scenario	89.10%	74.75%	79.64%
Sample Removal	84.58%	72.97%	77.01%
Simulation	77.07%	68.22%	67.15%
Instagram	63.30%	63.86%	72.54%
Facebook	76.44%	63.12%	74.67%
Pinterest	72.90%	61.85%	69.65%

grouped into three actual classes. These groups included mechanical classes (airplanes, automobiles, ships, trucks), small animals (birds, cats, frogs), and large animals (deer, dogs, horses).

In the first scenario,  $\mathcal{A}$  is aware of only these three classes, while the  $\mathcal{V}$  uses all 10 classes. In the second scenario,  $\mathcal{A}$  uses all 10 classes, while the  $\mathcal{V}$  uses only three classes. Since we observed a variance of 5% in the experiment results, each experiment was repeated 10 times. We observed that reducing the knowledge of the output space affects *Phantom*'s effectiveness. In the first scenario, *Phantom* reduced the accuracy in average by 4.4%, demonstrating that *Phantom* remains effective in this scenario. Notably, in the second scenario, no accuracy drop was observed, and *Phantom* was unable to reduce the accuracy.

This is likely because *Phantom* crafts the poisoning pattern using images with labels different from the original image, which causes the SSL algorithm to mislabel the images. However, if  $\mathcal{A}$  assumes a larger output space than  $\mathcal{V}$  actually uses, it is probable that the images of the poisoning pattern belong to the same class. For instance, if  $\mathcal{A}$  creates a poisoning pattern for an airplane using images of ships and trucks, and  $\mathcal{V}$  uses a reduced output space where these classes are grouped together into a superclass "mechanical items," the image will not be mislabeled during training. We will discuss this limitation further in Sect. 6.2.

In this section, we conducted a comprehensive evaluation of the effectiveness of the *Phantom* attack using six diverse datasets, showing its efficacy in distracting the training process diminishing the utility of the trained model, even for small PDRs. We evaluated the effects of various image augmentation techniques and potential counter measures, demonstrating the robustness of the *Phantom* attack. In a case study on 3 real-world social media platforms, we showed their susceptibility to *Phantom*, effectively demonstrating its effectiveness and the associated risks it entails.

## 6 SECURITY CONSIDERATIONS

In the preceding sections, we introduced the *Phantom* attack (Sect. 4) and evaluated it in various scenarios (Sect. 5). In this section, we will discuss the potential risks that the *Phantom* attack presents (Sect. 6.1), its limitations (Sect. 6.2), and possible future research direction (Sect. 6.3).

### 6.1 Impact of the *Phantom* Attack

The attack allows the adversary to degrade the performance of the model by simply uploading manipulated images to a platform with

user-generated content. The poisoned pattern introduced by the attack confounds the training algorithm, causing it to mislabel the manipulated images and resulting in the DNN model being trained with incorrect data. Thus, by uploading few manipulated samples, the *Phantom* attack affects not just a single model but all models being trained on these data.

Notably, the *Phantom* attack does not have strong requirements or assumptions. It is successful even with small Pattern Visibilities (PV), making it difficult to detect the manipulated images. The *Phantom* attack operates without any knowledge of the SSL algorithm, hyperparameters, or DNN architecture. Instead, the attacker simply uploads manipulated images to a platform with user-generated content, prior to the victim downloading the data and beginning the training process. This ability to poison the training without any knowledge of the attacked system highlights the increased attack surface created by utilizing data from untrusted sources without proper mitigation strategies. By uploading manipulated data, the attacker not only disrupts a specific SSL training procedure but also has the potential to prevent any SSL training for a particular task on the data from the affected platform. It is already sufficient to poison a small fraction of the data to achieve an accuracy drop between 5% and 10%. Notably, the uploading process could be also automated, as described in Sect. 6.2.

Even such small decreases in accuracy, such as a drop of 5% or 10% compared to the non-attacked model, can have serious consequences. For instance, in the context of self-driving cars, if a model fails to recognize the correct object, even in just 1% of the cases, this will cause the car to show wrong and potentially dangerous behavior in such situations, making the vehicle unusable. Similarly, in competitive scenarios, if two actors both train models but one model performs 10% better than the other model, the actor with the more accurate model will have an advantage in selling products based on their DNN models.

Also, the attack is not restricted to the image domain. The only requirement is the ability to combine a labeled sample with other samples, therefore, to overlay different samples weighted. This allows to combine the original samples with poisoning patterns. In Sect. 4.3, we described this exemplary for images. However, this can also be applied in other applications, such as applications that process audio files. Also here, different samples can be overlaid and the volume of the different samples can be used as Pattern Visibility (PV). Therefore, the *Phantom* attack is not restricted to image applications but is generally applicable.

Thus, the combination of low requirements and the ability to reduce the accuracy, the *Phantom* attack demonstrates the risk of untargeted poisoning attacks on SSL.

### 6.2 Limitations of the *Phantom* Attack

The *Phantom* attack does not require any prior knowledge of the training algorithm or the hyperparameters used, but it does necessitate some knowledge of the samples utilized for the labeled dataset. Adversaries can make educated guesses on the used labeled samples based on commonly available and publicly accessible datasets such as tiny images. In scenarios targeting a specific victim  $\mathcal{V}$ , the attacker could also incorporate knowledge obtained through data breaches or insider threats, which are not uncommon in industry.

However, as previously discussed in Sect. 3.2 the capability to make educated guesses is sufficient, as long as there is a degree of overlap between the guessed labeled samples  $\mathcal{X}_A$  and the actual labeled samples  $\mathcal{X}$ , i.e.,  $\mathcal{X}_A \cap \mathcal{X} \neq \emptyset$ . In Sect. 5.4, we evaluated scenarios where the adversary's guesses about the labeled images showed only a precision of 20%, thus, 20% of the images in  $\mathcal{X}_A$  were actually in  $\mathcal{X}$ . Further, we performed another experiment where the adversary increased the chance of having at least one correct guess per image by leveraging poisoning patterns that consist of 4 guesses for the labeled images. These experiments demonstrated that the ability to make educated guesses about the labeled dataset with a limited precision is sufficient for *Phantom* to significantly impact the model's accuracy.

In addition to the ability to make educated guesses on the labeled dataset, *Phantom* requires the adversary to be able to upload samples to the attacked platform. It might be a challenge here to control a considerable amount of samples. However, as shown in Sect. 5, *Phantom* is effective even with very small Poisoning Data Rates (PDRs). Notably, despite the social networks' significant efforts to identify and block automated content posting, bots continue to successfully upload content automatically [28, 36, 56, 58, 60], allowing an attacker to post automatically a certain fraction of manipulated media files. Furthermore, Carlini *et al.* recently demonstrated that significant portions even of established datasets can be manipulated with minimal effort [8], showing the practical applicability of *Phantom*.

Since the attack exploits the training algorithm's ability to predict wrong labels, it is restricted to Semi-Supervised Learning (SSL) settings. It is not applicable for pre-labeled scenarios like self-supervised learning that are used for text processing.

Further, in line with prior research on adversarial deep learning [4, 16, 33] and attacks on SSL in particular [7, 17, 19], also for the proposed attack, there is no formal proof to show that the attack works. To the best of our knowledge, all existing literature introducing attacks on SSL algorithms for DNNs show their effectiveness through an empirical evaluation. Consistent with this existing work, in Sect. 5, we presented an extensive empirical evaluation showcasing the effectiveness of our proposed *Phantom* attack across diverse datasets, SSL algorithms, input augmentation techniques, and attack parameter variations.

To craft the poisoning pattern, *Phantom* selects images with labels different from the original image. Therefore, *Phantom* requires knowledge on the output space. As observed in App. 5.7, the attack is ineffective if the attacker assumes a larger output space and, therefore, more labels than the victim actually uses. This occurs because *Phantom* uses samples with different labels to create the poisoning pattern, causing the SSL algorithm to mislabel them. However, if  $\mathcal{A}$  assumes a larger output space than  $\mathcal{V}$  uses, the samples of the poisoning pattern might belong to the same class in  $\mathcal{V}$ 's output space. Notably, the adversary can mitigate this risk by utilizing a reduced output space during the poisoning process. Therefore, the attacker needs to select images from classes that have a very high probability of belonging to different classes. For example, images from machines can be used to poison animal images. As shown in Sect. 5.7, this strategy allows the attack to remain effective even in case of a reduced output space.

Also, it should be noted that the *Phantom* attack is executed in a blind manner, without any assumptions regarding access or knowledge of the deployed algorithms, training process, or victims. However, this also introduces another challenge, as the adversary  $\mathcal{A}$  cannot monitor the attacked victim and, thus, cannot verify the success of the attack afterward. Analogous to other attacks against DNNs, such as inference attacks [49, 54], watermark removal strategies [9, 59], or poisoning attacks against self-supervised learning [31, 52, 53], the attacker can only measure the attack's effectiveness in a simulated environment. Consequently, it remains infeasible for the attacker to verify the attack's success for the actual victim, therefore, whether it's preventing DNN convergence (*Phantom* attack), confirming the utilization of extracted data for training (inference attacks), or validating the removal of an unknown watermark (watermark removal approaches).

### 6.3 Future Work

In our attack, we combined the original image with the poisoned pattern by performing weighted averaging to obtain the manipulated image. This enables the adversary to control the suspiciousness of the image using the PV parameter. Especially images that were crafted using low PV values seem to be inconspicuous to humans, particularly when they are displayed among many other benign images to the users of social media platforms. However, the question of what kind of adversarial perturbations are visible to humans is an active research topic [22, 50]. In this work, we focused on developing a scheme that combines two images and causes the SSL algorithm to use one for guessing the labels and the other for the actual training, resulting in mislabeled training samples. Therefore, the question on what kind of general patterns in images cause attention by humans or which combination of colors is prone to be easily-detectable is out of the scope of this work. Future work might improve the developed scheme and reduce the number of pixels, e.g., by removing the background of the labeled images that are used for the poisoning pattern. In this context, it should be emphasized that the adversary can still inspect the images before uploading them to ensure that they are inconspicuous.

### 6.4 Potential Counter Measures

In this paper, we introduced the *Phantom* attack that disrupts SSL training algorithms by uploading manipulated samples to the platform that is used as data source. We demonstrated the risks posed by *Phantom* through a case-study on three real-world social networks (see Sect. 5.6). An important research direction for future research is, therefore, to develop effective mitigation schemes against this type of attack.

We demonstrated in App. F that *Phantom* is robust against standard image augmentation techniques. Other defense strategies could involve adapting techniques that were developed against adversarial examples. Intuitively, the poisoning pattern that *Phantom* injects in the manipulated images might be comparable to the noise introduced by adversarial examples. Zantedeschi *et al.* propose applying Gaussian noise to the images to mitigate adversarial examples [65]. However, as we demonstrated in App. F, although applying Gaussian noise reduces the models' performance, *Phantom* remains effective. Pang *et al.* propose a thresholding test based

on a kernel density function to detect adversarial examples [43]. However, as shown in Sect. 5.5, the obtained scores for manipulated images are in the same range as for benign images. Also, a dedicated classifier was unable to detect the manipulated images (see Sect. 5.5). A key difference in an adversarial example that might be the reason for the ineffectiveness of these methods might be the fundamental difference in the patterns' structures. Adversarial examples exploit specific DNN parameter values to cause mispredictions, resulting in a random-like poisoning pattern. In comparison, the pattern of *Phantom* consists of real samples, thus showing structures and edges as regular samples do. Thus, further research is required to investigate potential countermeasures.

An important aspect for countermeasures against *Phantom* is the overlay of different samples and that the poisoning pattern is usually only weakly embedded (using low PV values). In the following, we describe two options that future work might investigate to remove the poisoning pattern by exploiting the overlay.

**Noise Reduction Techniques.** Signal processing methods, such as noise reduction, could be utilized for the removal of the poisoning pattern. A challenge here is to erase the pattern without affecting the algorithm's ability to process benign samples. Our evaluation demonstrated that simple compression and Gaussian smoothing are insufficient (see App. F) to mitigate the *Phantom* attack. Future research might, therefore, focus on more sophisticated signal-processing techniques, such as singular value decomposition [48], analyzing the samples in the frequency domain [24], or statistical analysis [34].

**Modeling Attack as Cocktail Party Problem.** The challenge of extracting the original sample from overlaid data in our scenario is similar to the well-known cocktail party problem. This problem describes a situation in which multiple audio signals overlap, similar to multiple conversations occurring simultaneously in a crowded room. Different approaches where proposed to separate signals using differential beamformers [10], transformer networks [57], or asynchronous fully recurrent convolutional neural networks [26]. Leveraging and adapting these techniques might provide a promising research direction to isolate and effectively separate the injected poisoning patterns from the original image while preserving the integrity of the original training samples.

## 7 RELATED WORK

In the following, we analyze existing work to attack SSL and untargeted attacks against deep learning. Despite the limited research on adversarial SSL, previous approaches focused on either injecting a backdoor into the resulting model or reducing the accuracy under the assumption that the adversary controls the labeled dataset. However, assuming control of the labeled dataset is not practical as it requires the adversary to control the victim. First, we will discuss existing attacks on SSL (Sect. 7.1), before describing several untargeted attacks against other, non-SSL, learning scenarios (Sect. 7.2).

### 7.1 Attacks on SSL

In previous research, various targeted poisoning attacks against SSL have been proposed, such as the white box backdoor attacks developed by Yan *et al.* [63, 64] and Feng *et al.* [17], which manipulate samples in the unlabeled dataset to cause the SSL algorithm to make

incorrect label predictions. They assume that the adversary can use the parameters of an intermediate version of the DNN model to determine a perturbation that causes the SSL algorithm to guess a wrong label for this specific sample. However, these assumptions are not practical, as this requires the adversary to be able to monitor the victim and the ongoing training process. However, if the adversary has access to the victim and can inspect the intermediate DNN model, there is no need to poison the unlabeled dataset but it can also poison, e.g., the labeled dataset. Neither is it practical to assume that the victim downloads the data a second time during the training. In comparison, *Phantom* does not require the adversary to have any control or any knowledge about the victim (parameters of the intermediate model, SSL algorithm, hyperparameters). It crafts the manipulated images once, before it is sufficient to upload the manipulated samples to the platform before the training is started (see Sect. 3.2).

Other studies [7, 12], focused on poisoning the unlabeled dataset by adding interpolations between samples from different classes to inject a backdoor into the trained DNN model. However, these attacks restrict the attack objective since they can only cause mispredictions for individual samples, rather than reducing the overall performance of the model (see Sect. 5.4). In contrast, *Phantom* significantly decreases the utility of the trained model and reduces its performance to that of a naive classifier, making the poisoned dataset unusable for SSL.

Franci *et al.* [19] and Liu *et al.* [32] perform both untargeted poisoning attacks by altering samples from the labeled dataset. They aim to minimize the number of labels that need to be changed to decrease the effectiveness of the models. However, this approach requires the attacker to have access to the labeled dataset, which implies a high level of capability for the attacker. An attacker that is able to control the small and manually labeled dataset of the victim is highly likely to be also able to interfere with the training process and directly sabotage the DNN model. In contrast, our proposed method only requires the attacker to upload manipulated samples to the source of the unlabeled dataset, such as a social network. Therefore, *Phantom* enables even a weak attacker to carry out poisoning attacks on semi-supervised learning and discourages the use of public data sources for SSL training.

### 7.2 Untargeted Poisoning Attacks against Other Learning Scenarios

In addition to SSL, untrusted data is also used in online learning scenarios, such as leveraging user feedback for predictions [44]. Several approaches have been proposed to address poisoning attacks in these scenarios by treating them as an optimization problem and creating samples that maximize the impact of the attack [27, 44, 67]. However, for online learning systems, the attacker can provide incorrect labels to confuse the system, and also has knowledge about the victim models, such as hyperparameters or even the weights. In contrast, *Phantom* is a black-box attack, in which the attacker has no knowledge of the DNN model or training algorithm.

Federated Learning (FL) is a distributed training approach where different clients perform the training locally and only share the parameters of their DNN models with a coordinating server [35]. The decentralized structure prevents the server from inspecting the



training data, thus making it vulnerable to untargeted poisoning attacks by malicious clients [6, 16]. However, these attacks typically involve knowledge of the current model's state, such as the current model parameters, and are, therefore, white-box attacks. Also, due to the decentralized training structure, the adversary can manipulate the model's parameters directly rather than being restricted to adding a few samples to the dataset as *Phantom* does.

## 8 CONCLUSION

In this paper, we presented *Phantom*, a novel untargeted-poisoning attack that disrupts Semi-Supervised Learning (SSL) training by introducing manipulated samples into the unlabeled dataset. While existing attacks on SSL either focus on backdoor attacks or require knowledge about the attacked training process, *Phantom* operates blindly. It crafts manipulated images before the training process starts without any knowledge about the training algorithm or hyperparameters. *Phantom* employs a combination of techniques that cause SSL algorithms to overlook the sample's actual content and instead rely on maliciously crafted patterns superimposed on real samples, leading to incorrect label guesses. Through a comprehensive evaluation, we demonstrated *Phantom*'s effectiveness on several state-of-the-art SSL algorithms, showing that it can be successful with small percentages of manipulated examples. Furthermore, we conducted a real-world case study to illustrate the vulnerability of data obtained from social networks, including Facebook, Instagram, and Pinterest, to *Phantom*.

Our work highlights the need for robust training algorithms that can effectively counteract untargeted-poisoning attacks in the context of SSL. Additionally, it emphasizes the importance of considering such attacks in the design and deployment of DNNs, particularly in sensitive domains such as social networks. Our results indicate that untargeted poisoning attacks on SSL can be effective and pose a serious threat to the security of DNNs. Therefore, it is crucial for researchers and practitioners to consider these types of attacks and develop appropriate countermeasures to secure DNNs.

## ACKNOWLEDGMENTS

This research received funding from the Horizon program of the European Union under grant agreements No. 101093126 (ACES) and No. 101070537 (CROSSCON), as well as the Federal Ministry of Education and Research of Germany (BMBF) within the IoTGuard project.

## REFERENCES

- [1] 2019. PyTorch. <https://pytorch.org>.
- [2] 2019. PyTorch - GTSRB. <https://pytorch.org/vision/0.17/generated/torchvision.datasets.GTSRB.html>
- [3] Wendy Kan Addison Howard, Eunbyung Park. 2018. ImageNet Object Localization Challenge. <https://kaggle.com/competitions/imagenet-object-localization-challenge>
- [4] Anish Athalye, Logan Engstrom, Andrew Ilyas, and Kevin Kwok. 2018. Synthesizing robust adversarial examples. In *ICML*. PMLR.
- [5] David Berthelot, Nicholas Carlini, Ian Goodfellow, Nicolas Papernot, Avital Oliver, and Colin A Raffel. 2019. Mixmatch: A holistic approach to semi-supervised learning. In *NeurIPS*.
- [6] Peva Blanchard, El Mahdi El Mhamdi, Rachid Guerraoui, and Julien Stainer. 2017. Machine learning with adversaries: Byzantine tolerant gradient descent. In *NIPS*.
- [7] Nicholas Carlini. 2021. Poisoning the Unlabeled Dataset of Semi-Supervised Learning. In *USENIX Security*. Usenix Association.
- [8] Nicholas Carlini, Matthew Jagielski, Christopher A Choquette-Choo, Daniel Paleka, Will Pearce, Hyrum Anderson, Andreas Terzis, Kurt Thomas, and Florian Tramèr. 2024. Poisoning Web-Scale Training Datasets is Practical. In *IEEE S&P*. IEEE Computer Society.
- [9] Xinyun Chen, Wenxiao Wang, Chris Bender, Yiming Ding, Ruoxi Jia, Bo Li, and Dawn Song. 2021. Refit: a unified watermark removal framework for deep learning systems with limited data. In *ACM Asia Conference on Computer and Communications Security*.
- [10] Zhuo Chen, Jinyu Li, Xiong Xiao, Takuya Yoshioka, Huaming Wang, Zhenghao Wang, and Yifan Gong. 2017. Cracking the cocktail party problem by multi-beam deep attractor network. In *2017 IEEE Automatic Speech Recognition and Understanding Workshop (ASRU)*. IEEE, 437–444.
- [11] Adam Coates, Andrew Ng, and Honglak Lee. 2011. An analysis of single-layer networks in unsupervised feature learning. In *AISTATS. JMLR Workshop and Conference Proceedings*.
- [12] Marissa Connor and Vincent Emanuele. 2022. Rethinking Backdoor Data Poisoning Attacks in the Context of Semi-Supervised Learning. *arXiv preprint arXiv:2212.02582* (2022).
- [13] Ekin D Cubuk, Barret Zoph, Dandelion Mane, Vijay Vasudevan, and Quoc V Le. 2019. Autoaugment: Learning augmentation strategies from data. In *IEEE/CVF Conference on Computer Vision and Pattern Recognition*.
- [14] Ekin D Cubuk, Barret Zoph, Jonathon Shlens, and Quoc V Le. 2020. Randaugment: Practical automated data augmentation with a reduced search space. In *IEEE/CVF Conference on Computer Vision and Pattern Recognition Workshops*.
- [15] Terrance DeVries and Graham W Taylor. 2017. Improved regularization of convolutional neural networks with cutout. In *arXiv preprint arXiv:1708.04552*.
- [16] Minghong Fang, Xiaoyu Cao, Jinyuan Jia, and Neil Gong. 2020. Local Model Poisoning Attacks to {Byzantine-Robust} Federated Learning. In *USENIX Security*.
- [17] Le Feng, Sheng Li, Zhenxing Qian, and Xinpeng Zhang. 2022. Unlabeled Backdoor Poisoning in Semi-Supervised Learning. In *IEEE International Conference on Multimedia and Expo (ICME)*. IEEE.
- [18] Hossein Fereidooni, Jan König, Phillip Rieger, Marco Chilese, Bora Gökbakan, Moritz Finke, Alexandra Dmitrienko, and Ahmad-Reza Sadeghi. 2023. AuthentiSense: A Scalable Behavioral Biometrics Authentication Scheme using Few-Shot Learning for Mobile Platforms. *NDSS* (2023).
- [19] Adriano Franci, Maxime Cordy, Martin Gubri, Mike Papadakis, and Yves Le Traon. 2022. Influence-driven data poisoning in graph-based semi-supervised classifiers. In *International Conference on AI Engineering: Software Engineering for AI*.
- [20] Jacob Gildenblat and contributors. 2021. PyTorch library for CAM methods. <https://github.com/jacobgil/pytorch-grad-cam>.
- [21] Ian J Goodfellow, Jonathon Shlens, and Christian Szegedy. 2014. Explaining and harnessing adversarial examples. *arXiv preprint arXiv:1412.6572* (2014).
- [22] Samuel Harding, Prashanth Rajivan, Bennett I Bertenthal, and Cleotilde Gonzalez. 2018. Human Decisions on Targeted and Non-Targeted Adversarial Sample.. In *CogSci*.
- [23] Charles R Harris, K Jarrod Millman, Stéfan J Van Der Walt, Ralf Gommers, Pauli Virtanen, David Cournapeau, Eric Wieser, Julian Taylor, Sebastian Berg, Nathaniel J Smith, et al. 2020. Array programming with NumPy. *Nature* 585, 7825 (2020), 357–362.
- [24] Hamid Hassani. 2008. A time–frequency approach for noise reduction. *Digital Signal Processing* 18, 5 (2008), 728–738.
- [25] Sebastian Houben, Johannes Stallkamp, Jan Salmen, Marc Schlipsings, and Christian Igel. 2013. Detection of traffic signs in real-world images: The German Traffic Sign Detection Benchmark. In *International joint conference on neural networks (IJCNN)*. IEEE.
- [26] Xiaolin Hu, Kai Li, Weiye Zhang, Yi Luo, Jean-Marie Lemerrier, and Timo Gerkmann. 2021. Speech separation using an asynchronous fully recurrent convolutional neural network. In *NeurIPS*.
- [27] W Ronny Huang, Jonas Geiping, Liam Fowl, Gavin Taylor, and Tom Goldstein. 2020. Metapoisn: Practical general-purpose clean-label data poisoning. In *NeurIPS*.
- [28] Stephanie Kirchaessner, Manisha Ganguly, David Pegg, Carole Cadwalladr, and Jason Burke. 2023. Revealed: The Hacking and disinformation team meddling in elections. <https://www.theguardian.com/world/2023/feb/15/revealed-disinformation-team-jorge-claim-meddling-elections-tal-hanan>
- [29] Alex Krizhevsky, Geoffrey Hinton, et al. 2009. Learning multiple layers of features from tiny images. Citeseer.
- [30] Y. Lecun, L. Bottou, Y. Bengio, and P. Haffner. 1998. Gradient-based learning applied to document recognition. *Proc. IEEE* 86, 11 (1998). <https://doi.org/10.1109/5.726791>
- [31] Chumeng Liang, Xiaoyu Wu, Yang Hua, Jiaru Zhang, Yiming Xue, Tao Song, Zhengui Xue, Ruhui Ma, and Haibing Guan. 2023. Adversarial Example Does Good: Preventing Painting Imitation from Diffusion Models via Adversarial Examples. In *ICML*. PMLR.
- [32] Xuanqing Liu, Si Si, Xiaojin Zhu, Yang Li, and Cho-Jui Hsieh. 2019. A unified framework for data poisoning attack to graph-based semi-supervised learning. *NeurIPS* (2019).
- [33] Yingqi Liu, Shiqing Ma, Yousra Aafer, Wen-Chuan Lee, Juan Zhai, Weihang Wang, and Xiangyu Zhang. 2018. Trojaning attack on neural networks. In *NDSS*.

- [34] Miguel Enrique Iglesias Martínez, Miguel Ángel García March, Carles Milián Enrique, and Pedro Fernández de Córdoba. 2022. *Algorithms for Noise Reduction in Signals: Theory and practical examples based on statistical and convolutional analysis*. IOP Publishing.
- [35] Brendan McMahan, Eider Moore, Daniel Ramage, Seth Hampson, and Blaise Agüera y Arcas. 2017. Communication-efficient learning of deep networks from decentralized data. In *AISTATS*. PMLR.
- [36] Cade Metz. 2020. Twitter bots poised to spread disinformation before election. <https://www.nytimes.com/2020/10/29/technology/twitter-bots-poised-to-spread-disinformation-before-election.html>
- [37] Yuval Netzer, Tao Wang, Adam Coates, Alessandro Bissacco, Bo Wu, and Andrew Y Ng. 2011. Reading digits in natural images with unsupervised feature learning. In *NIPS Workshop on Deep Learning and Unsupervised Feature Learning*.
- [38] Tuan Anh Nguyen and Anh Tuan Tran. 2021. WaNet-Imperceptible Warping-based Backdoor Attack. In *ICLR*.
- [39] Thanh Thi Nguyen, Quoc Viet Hung Nguyen, Dung Tien Nguyen, Duc Thanh Nguyen, Thien Huynh-The, Saeid Nahavandi, Thanh Tam Nguyen, Quoc-Viet Pham, and Cuong M Nguyen. 2022. Deep learning for deepfakes creation and detection: A survey. *Computer Vision and Image Understanding* 223 (2022), 103525.
- [40] OpenAI. [n. d.]. ChatGPT: Optimizing Language Models for Dialogue. <https://openai.com/blog/chatgpt/>.
- [41] OpenAI. 2023. Gpt-4 technical report. *arXiv preprint arXiv:2303.08774* (2023).
- [42] OpenAI. 2024. <https://openai.com/index/introducing-improvements-to-the-fine-tuning-api-and-expanding-our-custom-models-program>
- [43] Tianyu Pang, Chao Du, Yinpeng Dong, and Jun Zhu. 2018. Towards robust detection of adversarial examples. In *NIPS*.
- [44] Tianyu Pang, Xiao Yang, Yinpeng Dong, Hang Su, and Jun Zhu. 2021. Accumulative poisoning attacks on real-time data. In *NeurIPS*.
- [45] Billy Perrigo. 2023. OpenAI used Kenyan workers on less than \$2 per hour: Exclusive. <https://time.com/6247678/openai-chatgpt-kenya-workers>
- [46] Aditya Ramesh, Prafulla Dhariwal, Alex Nichol, Casey Chu, and Mark Chen. 2022. Hierarchical text-conditional image generation with clip latents. *arXiv:2204.06125* (2022).
- [47] Luke E Richards, André Nguyen, Ryan Capps, Steven Forsyth, Cynthia Matuszek, and Edward Raff. 2021. Adversarial transfer attacks with unknown data and class overlap. In *ACM workshop on artificial intelligence and security (AISec)*.
- [48] PK Sadasivan and D Narayana Dutt. 1996. SVD based technique for noise reduction in electroencephalographic signals. *Signal Processing* 55, 2 (1996), 179–189.
- [49] Ahmed Salem, Apratim Bhattacharya, Michael Backes, Mario Fritz, and Yang Zhang. 2020. Updates-Leak: Data set inference and reconstruction attacks in online learning. In *USENIX Security*.
- [50] Johannes Schneider and Giovanni Apruzzese. 2023. Dual adversarial attacks: Fooling humans and classifiers. *Journal of Information Security and Applications* 75 (2023), 103502.
- [51] Ramprasaath R Selvaraju, Michael Cogswell, Abhishek Das, Ramakrishna Vedantam, Devi Parikh, and Dhruv Batra. 2017. Grad-cam: Visual explanations from deep networks via gradient-based localization. In *IEEE international conference on computer vision*.
- [52] Shawn Shan, Jenna Cryan, Emily Wenger, Haitao Zheng, Rana Hanocka, and Ben Y Zhao. 2023. Glaze: Protecting artists from style mimicry by Text-to-Image models. In *USENIX Security*.
- [53] Shawn Shan, Wenxin Ding, Josephine Passananti, Stanley Wu, Haitao Zheng, and Ben Y Zhao. 2024. Nightshade: Prompt-Specific Poisoning Attacks on Text-to-Image Generative Models. In *IEEE S&P*. IEEE Computer Society.
- [54] Reza Shokri, Marco Stronati, Congzheng Song, and Vitaly Shmatikov. 2017. Membership inference attacks against machine learning models. In *IEEE S&P*. IEEE.
- [55] Kihyuk Sohn, David Berthelot, Nicholas Carlini, Zizhao Zhang, Han Zhang, Colin A Raffel, Ekin Dogus Cubuk, Alexey Kurakin, and Chun-Liang Li. 2020. Fixmatch: Simplifying semi-supervised learning with consistency and confidence. In *NeurIPS*.
- [56] Marianna Spring. 2024. Bot or not: Are fake accounts swaying voters towards Reform UK? <https://www.bbc.com/news/articles/c1335nj316lo>
- [57] Cem Subakan, Mirco Ravanelli, Samuele Cornell, Mirko Bronzi, and Jianyuan Zhong. 2021. Attention is all you need in speech separation. In *ICASSP 2021-2021 IEEE International Conference on Acoustics, Speech and Signal Processing (ICASSP)*. IEEE, 21–25.
- [58] Paul Tassi. 2023. I Never Had Bot Problems On Twitter Until Elon Musk, Now They're Stalking Me. <https://www.forbes.com/sites/paultassi/2023/12/29/i-never-had-bot-problems-on-twitter-until-elon-musk-now-theyre-stalking-me/>
- [59] Tianhao Wang and Florian Kerschbaum. 2019. Attacks on digital watermarks for deep neural networks. In *IEEE International Conference on Acoustics, Speech and Signal Processing (ICASSP)*. IEEE.
- [60] Samuel C. Woolley. 2020. *Bots and Computational Propaganda: Automation for Communication and Control*. Cambridge University Press, 89–110.
- [61] Cihang Xie, Mingxing Tan, Boqing Gong, Jiang Wang, Alan L Yuille, and Quoc V Le. 2020. Adversarial examples improve image recognition. In *IEEE/CVF Conference on Computer Vision and Pattern Recognition*.
- [62] Qizhe Xie, Zihang Dai, Eduard Hovy, Thang Luong, and Quoc Le. 2020. Unsupervised data augmentation for consistency training. In *NeurIPS*.
- [63] Zhicong Yan, Gaolei Li, Yuan Tlan, Jun Wu, Shenghong Li, Mingzhe Chen, and H Vincent Poor. 2021. Dehib: Deep hidden backdoor attack on semi-supervised learning via adversarial perturbation. In *AAAI conference on artificial intelligence*.
- [64] Zhicong Yan, Jun Wu, Gaolei Li, Shenghong Li, and Mohsen Guizani. 2021. Deep neural backdoor in semi-supervised learning: threats and countermeasures. *IEEE Transactions on Information Forensics and Security* 16 (2021), 4827–4842.
- [65] Valentina Zantedeschi, Maria-Irina Nicolae, and Amrbrish Rawat. 2017. Efficient defenses against adversarial attacks. In *ACM workshop on artificial intelligence and security*.
- [66] Bowen Zhang, Yidong Wang, Wenxin Hou, Hao Wu, Jindong Wang, Manabu Okumura, and Takahiro Shinozaki. 2021. Flexmatch: Boosting semi-supervised learning with curriculum pseudo labeling. In *NeurIPS*.
- [67] Xuezhou Zhang, Xiaojin Zhu, and Laurent Lessard. 2020. Online data poisoning attacks. In *Learning for Dynamics and Control*. PMLR.

## A IMAGE AUGMENTATION

Data augmentation is a technique that modifies the individual samples of training data, being used, e.g., to create a larger dataset for training DNNs.

One common example of data augmentation is the use of image mirroring, where the image is flipped horizontally. This technique is particularly useful in increasing the diversity of the training dataset and thereby increasing the robustness and generalization ability of the DNN. By requiring the DNN to learn features that are invariant to horizontal flipping, the model is encouraged to focus on important features of the image and not on the specific orientation of the image. This in turn, improves the model's ability to generalize to new, unseen images. Additionally, this technique also increases the number of training examples and can help reduce overfitting. As we will further explain in Sect. 2.1, certain algorithms for SSL utilize data augmentation to improve the DNN's generalization ability [13, 15, 61]. We categorize data augmentation techniques into two groups:

### Weak augmentation

techniques make minimal modifications to the training samples, such that the colors and shapes are preserved. Examples of such techniques include horizontally flipping the images along the center axis and randomly shifting the images by a small number of pixels.

### Strong augmentation

involves significant modifications, such as altering the color or obscuring parts of the image. One example of a strong data augmentation technique used by SSL algorithms is RandAugment [14], which employs techniques such as image inversion and partial image occlusion. These modifications can make it challenging even for humans to correctly identify the class of the augmented image [13].

## B ETHICAL CONSIDERATIONS

In Sect. 5.6, the effectiveness of our attack on data that were obtained from different real-world social networks is demonstrated. To conduct these experiments, manipulated images were uploaded to three different social networks: Facebook, Instagram, and Pinterest. The effectiveness of our attack was evaluated using the manipulated data from these social networks. To ensure that these experiments do not have any negative impact on anyone, careful consideration and adaptation of the privacy settings for the profiles on each social network were applied. We created on Facebook a private album

that only we could access, on Instagram a private account with no followers, and on Pinterest a secret board was created.

In the present study, particular attention was given to the privacy settings on three popular social media platforms, namely Facebook, Instagram, and Pinterest. For Facebook, the "Select audience" option in the privacy settings was configured to "Only me," thereby ensuring that the visibility of the posted content was limited to the account holder alone. For Instagram, the account policy was set to "Private Account" and the account was not connected to any other account, thereby ensuring that the content was not accessible to others. On Pinterest, the option to "Hide your profile from search engines (e.g., Google)" was enabled, and a secret board was created to upload all images. Additionally, none of the accounts was connected to any other account, thus ensuring that the images remained private.

As a precautionary measure, the content and corresponding user accounts were immediately deleted after downloading them. Each of the social networks stated that deleting the account would also result in the deletion of any stored data. Furthermore, we carefully analyzed the usage terms of each of the social networks utilized in the study and ensured that conducting the experiments did not violate them. The experiments were also aligned with the ethical guidelines of the involved research institutions.

### C FOCUS OF SSL ALGORITHMS ON LABELED DATASET

The focus of SSL algorithms on the labeled dataset during the early stages of training is an important factor that is exploited in our proposed untargeted-poisoning attack. When training begins with randomly initialized parameters, the guessed labels have low accuracy, making the labeled samples the only source of truth. This results in the DNN overfitting on these samples. Figure 7 shows the accuracy on the labeled dataset, the unlabeled dataset<sup>4</sup>, and the test dataset during training for all three SSL algorithms (MixMatch, UDA, FixMatch) in a scenario without attack. As the figure shows, all three algorithms achieve an accuracy of 100% on the labeled dataset within 4 epochs, while the accuracy on the unlabeled dataset takes significantly longer to converge.

<sup>4</sup>For the accuracy calculation we used the labels for those images, which are unknown to the training algorithm.

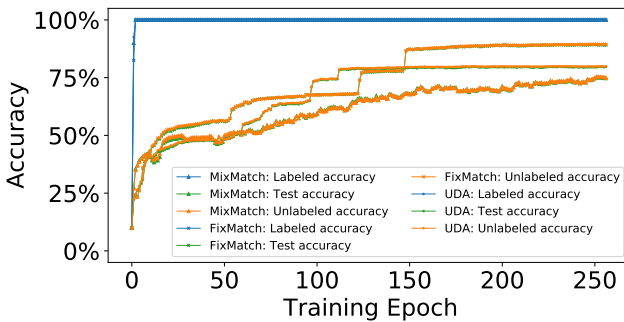


Figure 7: Performance of the DNN for the labeled dataset  $\mathcal{X}$ , unlabeled dataset  $\mathcal{U}$  and test dataset during training.

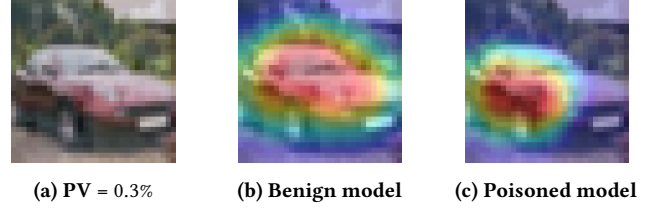


Figure 8: GradCAM of a benign and a poisoned model.

Our proposed attack takes advantage of this observation by hiding parts of labeled images in some unlabeled images, which causes the overfitted DNN to mispredict the labels for these images based on the hidden labeled images. By exploiting the focus of SSL algorithms on the labeled dataset, *Phantom* is able to disturb the training process and lead to incorrect label guesses.

### D ANALYSIS OF MODEL BEHAVIOR

In order to thoroughly analyze how the *Phantom* attack manipulates the model's behavior, we analyze the saliency map, which illustrates the model's attention. This methodology enables us to compare the model's attention between the benign and poisoned models, thereby providing insight into the attack's impact on the model. For plotting the saliency maps, we employed the widely used GradCam approach [51] and utilized the implementation of Gildenblat *et al.* [20].

Figure 8 shows the saliency maps for a benign and a poisoned model. The saliency map of the benign model reveals that the model's decision-making process is based on the analysis of the whole object, as can be observed in Fig. 8b. In contrast, the saliency map of the poisoned model illustrates the model's attention is primarily focused on the image's right side, where one of the labeled images for the poisoning pattern is located. This can be attributed to the fact that the poisoned model was trained on both the pattern and the car image, while the benign model was only trained on recognizing the car. As a result, the center of attention is shifted to the left for the poisoned image, indicating overfitting on the data. The shift in attention highlights the impact of the poisoning pattern in the manipulated images and *Phantom*'s effectiveness.

### E CHOICE OF DENSITY FUNCTIONS IN BACKDOOR ADAPTION

In the past, different security attacks on SSL have been proposed [7, 12] that aim to inject a backdoor into the model. In comparison to these attacks, does not inject additional functionality into the model but disturbs the ability to utilize the non-manipulated data, which creates several significant challenges, as discussed in Sect. 3.3. In Sect. 5.4, we compared the *Phantom* attack against different baseline attacks, including an adaption of the attack proposed by Carlini [7]. The attack interpolates between samples of two classes that the attack aims to connect, i.e., making the model classify samples of one class as samples of the second class. In Tab. 5, we showed only the results for the density function  $1.5 - x$ , that is, according to Carlini [7] the most effective density function. For the sake of completeness, we show in Tab. 9 the results for other

**Table 9: Effectiveness of density functions for an untargeted version of the attack proposed by Carlini [7] for a PDR of 10%.**

Density Function	UDA
Benign Scenario	79.64%
Remove 10% of Samples	77.01%
$1 - x^2 + 0.5$	82.47%
1	85.96%
$1 - x$	82.92%
$1.5 - x$	81.03%
<i>Phantom</i> (PV=0.2, PDR=10%)	67.15%
<i>Phantom</i> (PV=0.1, PDR=5%)	68.71%

density functions. As the table shows, *Phantom* is more effective than any of these density-function-based attacks, while the density functions works as regularization and, in consequence, sometimes even remove the model’s utility.

## F FURTHER EVALUATION

In real-world applications, typically, data preprocessing techniques might be applied to improve computation efficiency, e.g., through data compression to reduce necessary storage size. Other preprocessing techniques can involve image augmentation to improve the performance of the trained model. To evaluate the practical applicability of *Phantom*, we, therefore, conducted several experiments involving various data-augmentation methods (Gaussian smoothing, JPEG compression, and random image rotation) to assess *Phantom*’s robustness against these techniques. The evaluation is conducted with a PDR of 5% and a PV of 0.1. As the results in Tab. 10 show, although the data augmentation impacts model performance even in the absence of an attack, *Phantom* is still able to reduce the model’s utility. Notably, image flipping, an augmentation technique that horizontally flips the original image, is already part of the weak augmentation methods applied in SSL algorithms. Consequently, this technique was included in all our experiments, and no additional tests were conducted for it.

Furthermore, we assessed the effect of compression on *Phantom* as part of our case study (see Sect. 5.6). The reason for this assessment is that compression can affect the quality of the images and, thus, the performance of the algorithms that operate on them. By evaluating the effect of compression on *Phantom*, we aimed to investigate its robustness to this kind of degradation of the input data.

Table 11 shows the effectiveness of *Phantom* for very low PDRs. As the table shows, even for small PDRs, *Phantom* reduces the accuracy by 10% for FixMatch and 5% for UDA and MixMatch. Thus MixMatch and UDA seem to be more robust against very

small fractions of manipulated data. Notably, for a PDR of 3%, the accuracy is reduced by almost 10%, showing that *Phantom* is still effective.

**Table 10: Effectiveness of *Phantom* for the CIFAR-10 dataset for different data augmentation techniques.**

Augmentation	FixMatch		MixMatch		UDA	
	Benign	Attack	Benign	Attack	Benign	Attack
No Augmentation	89.10	83.68	74.75	64.85	79.64	68.71
Gauss. Smoothing	91.98	76.21	71.45	68.43	79.53	70.53
Random Rotation	82.99	72.05	63.82	61.95	83.28	77.58
JPEG Compression	87.75	74.12	74.25	69.92	83.05	73.48

**Table 11: Effectiveness of *Phantom* for very low Poisoned-Data-Rates (PDRs) for the CIFAR-10 dataset.**

PDR	FixMatch	UDA	MixMatch
0.0% (No-Attack)	89.10 %	79.64 %	74.75 %
0.1%	77.78 %	73.93 %	72.71 %
0.5%	79.43 %	72.41 %	69.83 %
3.0%	78.74 %	72.66 %	65.13 %
5.0%	83.68 %	68.71 %	64.85 %